

3-D refraction tomography: a tool for interpretation of WARP data

Pavel *Ditmar**, Hamburg University; Harry Mack: Mobil Technology Corp.;
and Jannis Makris, Hamburg University

Summary

A technique for inversion of 3-D WARP data into a 3-D depth-velocity model has been developed. The model is assumed to consist of several layers separated by interfaces. The velocity structure of each layer is laterally homogeneous; but the depth of each interface may vary. The input information is traveltimes of refracted (turning) P-waves. Potential of the technique is illustrated by an example of real data interpretation.

Introduction

Presently: WARP is well-known as a 2-D seismic method. There are various approaches to interpretation of 2-D WARP data: "trial-and-error" method, when differences between observed and calculated traveltimes are minimized manually (*Makris*, 1995); tomographic inversion (*Zelt and Smith*, 1992; *Ditmar and Makris*, 1996); refracted wave migration (*Pilienko and Makris*, 1997). 2-D WARP may also be used for areal studies: several parallel or intersecting profiles should be deployed in this case. The set of individual 2-D models is then interpolated into the final 3-D model. To eliminate the necessity of bringing 2-D models into the coincidence at the profile intersections, the set of models may be produced simultaneously (*Zelt*, 1994). But one could expect that consideration of a truly 3-D geometry would furnish better results, because shot-to-receiver pairs belonging to different profiles are included in the interpretation in this case. Thanks to that, the amount of information about the model increases: illumination of the model becomes more comprehensive.

We developed an interpretation technique for 3-D WARP data. by concentrating on refracted (turning) P-waves, since in the majority of WARP experiments, refracted waves are mostly observable and suitable for interpretation. We called our technique "refraction tomography", by analogy to the reflection tomography" designed for interpretation of conventional seismic data. Refraction tomography is also aimed at restoring both interface configurations and seismic velocities. By now our technique is limited to the case of laterally homogeneous velocities. In the future, it may be generalized to more complicated models.

Theory

We assume that the model consists of several layers, separated by interfaces. Configuration of each interface is

described via a rectangular grid; interface depth between grid nodes' is determined by bi-linear interpolation. The velocity in each layer is horizontally homogeneous. It is determined by values at two different depth levels. Thus, it may possess constant vertical gradient. The two basic steps of tomographic inversion are: (1) tracing of seismic rays in the initial model and (2) inversion itself.

Ray-tracing. Our algorithm for tracing refracted waves is based on the assumption that interfaces do not contain steep areas (the angle between the normal to the interface and the vertical line is everywhere small). To begin with, let us consider an 1-D medium consisting of several homogeneous layers separated by perfectly flat interfaces. Such a medium produces a set of head waves: raypaths of which may be calculated easily. This is thanks to the fact that each raypath in a 1-D medium is characterized by a constant parameter $p = 1/V_R$, where V_R is velocity in the refracting layer (the head wave propagates along its top). Ray-tracing in a 1-D medium when velocities are characterized by vertical gradients: is a bit more difficult. In this case, each layer with a monotonically changing velocity may be approximated by a set of thin layers with constant velocities. Ray-tracing should be carried out for each of these thin layers. Finally, the calculated traveltimes are compared: the resulting ray is the one with the minimum traveltime.

Now, let us proceed to our case, when velocities are horizontally homogeneous: but interfaces are not perfectly flat. Our key assumption is that the medium is 1-D locally. It means that the depth of each interface for tracing the downgoing branch is taken as that at the point where the ray crosses the interface; the same is true when the upgoing branch is traced (fig.1). Naturally: exact depths of crossing points are unknown until the ray-tracing is finished. But the computations may be organized iteratively. Originally, the 1-D model to trace the downgoing branch is constructed of depths just below the source and the one to trace the upgoing branch is constructed of depths just below the receiver. The original ray parameter is taken as the reciprocal average velocity in the refracting layer. Then the seismic ray is traced. After that, the local 1-D models and the ray parameter may be refined. The iterative process is stopped, when the difference between calculated traveltimes at two successive iterations is sufficiently small. Finally, part of the raypath belonging to the refracting layer is analyzed: the ray is considered as not existing if some points of this part are outside of the

3-D refraction tomography

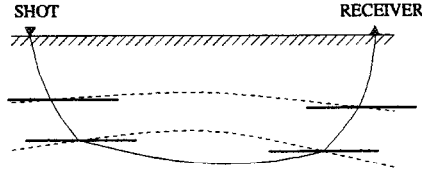


Figure 1: An illustration to the notion of “locally 1-D medium”. Dashed lines are true interfaces; thick solid lines are elements of the locally 1-D model; thin solid line is the raypath.

refracting layer due to interface undulations.

Inversion. The purpose of the inversion step is to calculate a refined model, fitting the observed traveltimes better than the initial one. Optionally, some extra unknown parameters may be found jointly with the refined model, such as shot time delays. An additional time delay calculated for each shot accounts for: (1) inaccuracy of the shot time; (2) time interval between the signal beginning and the intensive phase to be picked; (3) small-scale heterogeneities below the shot point. Calculation of shot time delays is an important feature of our inversion algorithm: otherwise non-accounted time delays cause false depth anomalies near shot points.

The necessary input information for inversion is the set of observed (picked) traveltimes together with relevant raypaths and traveltimes calculated in the ray-tracing step. Raypaths are necessary for calculation of the partial derivative matrix. Calculated traveltimes are used to compute traveltime residuals (differences between observed and calculated traveltimes). The partial derivative matrix together with the set of traveltime residuals are parameters of the objective function, which should be minimized for obtaining the refined model=

$$\Phi(\mathbf{m}) = (\mathbf{A}\Delta\mathbf{m} - \Delta\mathbf{T})^T (\mathbf{A}\Delta\mathbf{m} - \Delta\mathbf{T}) + \alpha\mathbf{R},$$

where A is the matrix of partial derivatives:

$$A_{ij} = \left. \frac{\partial T_i(\mathbf{m})}{\partial m_j} \right|_{m_j = m_j^{init}} ;$$

\mathbf{m} is the vector of all unknown parameters; $\Delta\mathbf{m} = \mathbf{m} - \mathbf{m}^{init}$ is the difference between the the perturbed vector of unknown parameters and the initial one; $\Delta\mathbf{T}$ is the vector of traveltime residuals; \mathbf{R} is a regularization condition; α is regularization parameter. To minimize the objective function, we make use of the conjugate gradient method.

The regularization condition we propose is the requirement that the refined interfaces should be as smoothed as

possible. For simplicity, we present it here in the integral form, bearing in mind that its finite-difference analog is actually used:

$$R = \sum_k \iint \left[\left(\frac{\partial(Z_k - Z_k^{init})}{\partial x} \right)^2 + \left(\frac{\partial(Z_k - Z_k^{init})}{\partial y} \right)^2 \right] dx dy,$$

where $Z_k = Z_k(x, y)$ is the refined configuration of interface number k (unknown); $Z_k^{init} = Z_k^{init}(x, y)$ is the initial configuration of interface number k ; the summation is over all interfaces to be refined.

Naturally, the result of the objective function minimization may be treated as the final model, only if it differs from the initial one not very considerably. Otherwise the non-linearity of the problem should be taken into account. It means that the final model is to be found iteratively: the result of inversion is specified as the new initial model, then new ray-tracing and inversion are carried out etc.

Example

Data. The developed interpretation technique was applied to WARP data, collected in the Iquitos area, Peru. Shots and receivers were distributed along four parallel profiles, as presented in the fig.2. The length of each profile was 41 km; the distance between neighbour profiles comprised 3.5 km, whereas the geophones were situated approximately 250 m apart. On each of the four profiles, 14 shots were made approximately 3 km apart. The shots on the first profile were recorded by all receivers. The shots on the second profile were recorded by receivers on profiles 1 and 2, the shots on the profile 3 were recorded by receivers on profiles 1 and 3, and the shots on the profile 4 were recorded by receivers on profiles 1 and 4.

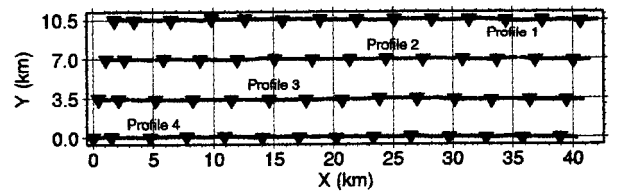


Figure 2: Disposition of profiles and shots (triangles).

After a preliminary analysis of the collected information, the presence of three main layers was established: top sedimentary layer with approximate velocity $V_p=2$ km/s; bottom sedimentary layer ($V_p=2.8$ km/s); basement ($V_p=6$ km/s). The traveltimes of relevant seismic arrivals were picked. The total number of picked data comprised 12215 (9898 of picked events were identified as the refraction in the basement: 1759 as the refraction in the bottom sedimentary layer and 558 as the direct wave).

3-D refraction tomography

	Depth (km)	Depth 1 (km)	Vel.1 (km/s)	Depth 2 (km)	Vel.2 (km/s)
Layer 1 (Top sediment. layer)	-	-0.3	2.11	1.0	2.22
Interf.2	0.31	-	-	-	-
Layer 2 (Bottom sediment. layer)	-	0.0	2.70	2.0	2.90
Interf.3	1.50	-	-	-	-
Layer 3 (Base-ment)	-	1.0	5.94	4.0	6.13

(but realistic) perfectly flat model. We applied the tomographic technique as it was described above, but keeping the model flat. The result is presented in table 1. This model was then used as the initial guess in the second step, when detailed interface configurations were calculated. The final model is shown in table 2 and fig.3.

	Depth (km)	Depth 1 (km)	Vel.1 (km/s)	Depth 2 (km)	Vel.2 (km/s)
Layer 1	-	-0.3	2.16	1.0	2.27
Interf.2	fig.3a	-	-	-	-
Layer 2	-	0.0	2.74	2.0	2.93
Interf.3	fig.3b	-	-	-	-
Layer 3	-	1.0	5.92	4.0	6.21

Table 1: The model after the first interpretation step (The initial model for tomographic inversion).

Table 2: The final model.

Interpretation. The interpretation consisted of two steps. In the first step, we started from an arbitrary

Results. The derived interface configurations show a clone correlation. In the left part of the investigated region ($0\text{km} < X < 7\text{km}$), the interfaces are relatively shallow:

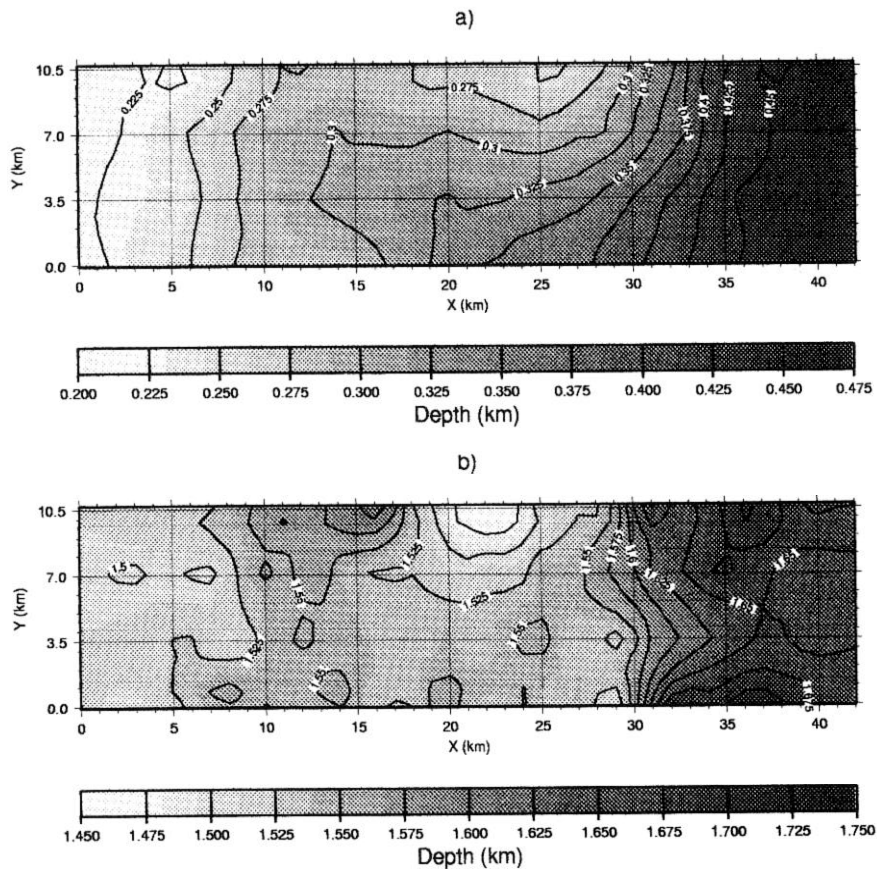


Figure 3: The final model. (a) configuration of the interface 2 (inter-sedimentary interface); (b) configuration of the interface 3 (top of the basement).

3-D refraction tomography

the depths are equal to 225-250m and to 1500-1525m for interfaces 2 and 3, respectively. In the middle part (7km < X < 30km): the interfaces are found at an intermediate depth: 275-350m and 1525-1575m. Both interfaces reveal a local uplift at the vicinity of profile 1, where the depth of interfaces 2 and 3 decreases to 250 and 1450m, respectively. To the right from the line X=30km, both interfaces are located deeper. The depth of interface 2 increases to the right gradually, so that at the right edge of the area it reaches 470m. The relief of interface 3 looks less smoothed. There is evidence of a fault: crossing all four profiles approximately at X=30km. In the right part of the area, the prevailing depth of the interface 3 is 1650m. At the vicinity of profiles 1 and 4 the depth increases even more: up to 1700-1720m.

Illumination of the model. Each picked traveltime controls the interface above the refracting layer at two points: where the ray enters the refracting layer and where the ray departs from it. We call these points "refraction points" by analogy with "reflection points": controlling interface depth in reflection tomography. The map of refraction point allows one to understand how well different areas of the model are controlled by the data picked. We have prepared maps of refraction points for interfaces 2 and 3 (fig.4), using raypaths calculated for the initial model (table 1). One can see that interface depths below the profiles are well constrained. Moreover, refraction points extend for a certain distance from profiles: 650 m for the interface 2 and 800 m for the interface 3. This is due to the fact that 3-D data were included into the interpretation when shots and receivers belonged to different profiles.

Accuracy of inversion results. To estimate the accu-

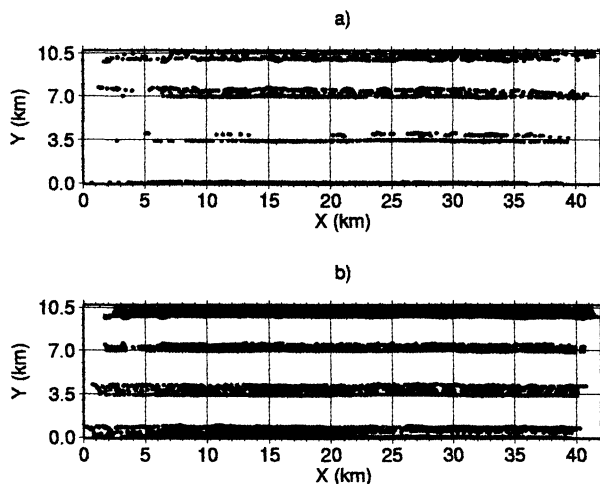


Figure 4: Disposition of refraction points for interfaces 2 (a) and 3 (b).

racy of inversion, we split the picked data into two parts, accordingly to shot numbers: odd shots data and even shots data. Then the tomographic inversion was repeated for the two data sets independently. The obtained models showed a good agreement with each other and with the one produced from all data. The rms misfit between interfaces in the two models on one hand and interfaces presented in fig.3 on the other comprised 21-28 m for the interface 2 and 11-15 m for the interface 3.

Conclusion

We have shown that a 3-D WARP experiment evaluated with the presented interpretation technique may give an exact image of the interface configurations, provided that the medium is not very inhomogeneous laterally. To achieve a good control over the model, we recommend to make use of a dense 2-D grid of receivers. On the other hand, there is no need for a big number of shots. In principle, just a few could be enough, provided the generated waves approach the receivers at different *azimuths*. For example, these shots may be located along the perimeter of the investigated area. Naturally: that is true only for not very complicated models, when the lateral velocity variations are negligible and seismic arrivals in all sections may be easily identified. Another limitation is caused by the fact, that arrivals of a specific origin are often visible only within a limited interval of shot-to-receiver distances. Therefore: the spacing of shot lines inside the investigated area should be increased, if shallow interfaces are to be mapped. It goes without saying, that the inverse observation geometry may be used: a dense grid of shots and a limited number of receivers.

References

- Ditmar.P.G. and Makris,J.. 1996, Tomographic inversion of 2-D 'WARP data based on Tikhonov regularization: *66th Ann. Internat. Mtg., Soc. Expl. Geophys., Expanded Abstracts*, p. 2015-2018.
- Makris,J., 1995: Wide Angle Reflection Profiling - applications for petroleum exploration and crustal studies: Paper presented at 11th *Geophysical Conference and Exhibition of ASEG*, 3-6 September 1995, Adelaide Convention Centre and Exhibition Hall Adelaide, South Australia
- Pilipenko,V. and Makris,J., 1997: Refracted wave migration: *59th EAGE Conf. and Techn. Exhib., Extended Abstracts* (in press)
- Zelt.C.A.. 1994: 3-D velocity structure from simultaneous traveltime inversion of in-line seismic data along intersecting profiles: *Geophys.J.Intl.* 118, p-795-801.
- Zelt, C.A. and Smith,R.B., 1992. Seismic traveltime inversion for 2-D crustal *velocity structure: Geophys.J.Int.*, 108, p.16-34.